Thermochemistry of the Chromium Hydroxides $Cr(OH)_n$, $n = 2-6$, and the Oxyhydroxide $CrO(OH)_4$: Ab Initio Predictions

Ida M. B. Nielsen* and Mark D. Allendorf

Sandia National Laboratories, P.O. Box 969, Livermore, California 94551

Received: November 8, 2005; In Final Form: January 26, 2006

We here present a high-level ab initio study of the thermochemistry of the chromium hydroxides $Cr(OH)_n$, $n = 2-6$, and of the oxyhydroxide $CrO(OH)_4$. Optimum geometries and harmonic vibrational frequencies were determined at the B3LYP level of theory using basis sets of triple-ζ quality including polarization and diffuse functions. Heats of formation were obtained from isogyric reaction energies computed at the CCSD(T) level of theory using large basis sets and including corrections for core-valence correlation, scalar relativistic effects, and basis set incompleteness. Additionally, polynomial fits were performed for the heat capacity and the standard enthalpy and entropy over the 100−3000 K temperature range. While our computed heats of formation agree well with previously obtained experimental data for some of these species, our results suggest that revision of the experimental data for others may be appropriate.

1. Introduction

The corrosion of chromium-containing materials at high temperatures involves the formation of a potentially large number of volatile species. Understanding the chemistry of this corrosion is important for both environmental and technological reasons. Health issues associated with the volatilization of Cr(VI) species in waste incinerators have long been a concern. In addition, the loss of chromium in the presence of air and water vapor is a key roadblock in the development of interconnects for solid oxide fuel cells,[1,2] which use chromium-containing alloys, and refractories. The use of alloys containing chrome also leads to catalyst poisoning in steam-methane reformers by deposition of chromium oxides,[3] and volatile chromium species formed in atmospheric pressure chemical vapor deposition reactors used in the semiconductor industry can contaminate processed wafers, causing increased defect rates.[4]

Unfortunately, experimental data for these species is often unavailable or conflicting, leading to very high uncertainties in the predictions of models developed to understand the corrosion process. Computational approaches can help resolve inconsistencies among experimental data and fill gaps in the knowledge base. Recently, we used coupled-cluster methods and large basis sets to determine thermochemical data for chromium halides.[5] The agreement between the limited experimental data available and the predicted heats of formation is generally good, lending confidence to the overall theoretical approach. We have also extended these methods to $CrO_2(OH)_2$, a key species in the volatilization of Cr_2O_3 by steam,[6] and obtained reasonable agreement between experimental and theoretical equilibrium constants over the 500−800 °C temperature range.

In the present work, we investigate the chromium hydroxides $Cr(OH)_n$, $n = 2-6$, and the oxyhydroxide $CrO(OH)_4$ for which most of the previously reported heats formation are not well-established. Available thermochemical data for these compounds are listed in Table 1. Ebbinghaus[7] presented experimentally derived thermodynamic data for gas-phase chromium species, including all of the hydroxides and oxyhydroxides studied in the present work. Because of the lack of experimental data for these species, their heats of formation were estimated from the heats of formation for chromium halides and oxyhalides by using various assumptions of linear relationships between bond strengths for different ligands. In a later study, Ebbinghaus[8] reevaluated the heats of formation for several chromium halides and oxyhalides and used these results to obtain revised values for the heats of formation for many of the chromium hydroxides and oxyhydroxides. A theoretical study by Espelid et al.[9] computed bond dissociation energies and heats of formation for several chromium hydroxides and oxyhydroxides but included only one species, $Cr(OH)_2$, from the present study. The two methods employed were CCSD(T)-based variants of the G2 procedure and the PCI-X scheme for scaling correlation energies,[10] and these methods were in excellent agreement for the smaller species investigated, including $Cr(OH)_2$, although rather large discrepancies were obtained for some of the larger compounds studied.

TABLE 1: Previously Determined $\Delta H^\circ_{f,298.15}$ Values for Gaseous $Cr(OH)_n$, $n = 2-6$, and $CrO(OH)_4$

species	$\Delta H^\circ_{f,298.15}$ (kcal mol^{-1})
$Cr(OH)_2$	-78.1 ± 2.6,[a] -73.9 ± 2.9[b]
$Cr(OH)_3$	-145.7 ± 3.1[a]
$Cr(OH)_4$	-202.9 ± 3.5[a]
$Cr(OH)_5$	-218[a,c]
$Cr(OH)_6$	-229[a,c]
$CrO(OH)_4$	-220[a,c]

[a] From ref 8. [b] From ref 9. [c] Lower bound.

We here employ high-level ab initio methods to compute the heats of formation and thermodynamic functions for the chromium hydroxides $Cr(OH)_n$, $n = 2-6$, and the oxyhydroxide $CrO(OH)_4$. Structures and harmonic vibrational frequencies are computed with density functional theory, and heats of formation are obtained from isogyric reaction energies computed using coupled-cluster theory, including corrections for basis set incompleteness, core-valence correlation, and scalar relativistic effects. Additionally, thermodynamic functions are computed

* To whom correspondence should be addressed. E-mail: ibniels@ca.sandia.gov.

10.1021/jp0564546
Published on Web 02/22/2006

TABLE 2: Thermochemical Data (kcal mol^{-1}) from the Literature Employed in the Computation of Heats of Formation in the Present Work

species	$\Delta H^\circ_{f,0}$	$\Delta H^\circ_{f,298.15}$
Cr(g)	94.49 ± 1.0^a	95.00 ± 1.0^a
CrOH(g)	16.7 ± 1.4^b	16.3 ± 1.4^c
CrO_3(g)	-76.4 ± 1.0^d	-77.3 ± 1.0^e
H_2O(g)	-57.103 ± 0.010^a	-57.798 ± 0.010^a

[a] From ref 38. [b] Computed from the reaction Cr(s) + $0.5O_2$(g) + $0.5H_2$(g) → CrOH(g) using the $\Delta H^\circ_{298.15}$[CrOH(g)] value from ref 9 and the $H^\circ_{298.15} - H^\circ_0$ values from ref 7. [c] From ref 9. [d] Obtained from the reaction Cr(s) + $1.5O_2$(g) → CrO_3(g) using the $\Delta H^\circ_{298.15}$[CrO_3(g)] and $H^\circ_{298.15} - H^\circ_0$ values given in ref 7. [e] From ref 7.

over a range of temperatures, and polynomial coefficients in the CHEMKIN format[11] are reported.

2. Computational Details

Heats of formation were computed using the following set of isogyric reactions

$$Cr(OH)_2 + Cr \rightarrow 2CrOH \quad (1)$$

$$Cr(OH)_3 + 2Cr \rightarrow 3CrOH \quad (2)$$

$$Cr(OH)_4 + 3Cr \rightarrow 4CrOH \quad (3)$$

$$Cr(OH)_5 + CrOH \rightarrow CrO_3 + Cr + 3H_2O \quad (4)$$

$$Cr(OH)_6 \rightarrow CrO_3 + 3H_2O \quad (5)$$

$$CrO(OH)_4 \rightarrow CrO_3 + 2H_2O \quad (6)$$

In addition to the target chromium hydroxides and oxyhydroxide, these reactions involve only small auxiliary species (H_2O, atomic chromium, CrOH, and CrO_3) with relatively well-established heats of formation. For $Cr(OH)_6$ and $Cr(OH)_5$, reactions analogous to reactions 1−3 were also investigated but were discarded because the CCSD → CCSD(T) shifts in the reaction energies (vide infra) were very large. Reaction energies were computed at 0 K and converted to 298.15 K by application of computed temperature corrections (vide infra). Heats of formation were obtained using the computed reaction energies and the heats of formation for Cr, CrOH, CrO_3, and H_2O listed in Table 2.

For all species in reactions 1−6, optimum geometries and harmonic vibrational frequencies were computed with the B3LYP density functional method (unrestricted for open-shell species) using the 6-311++G(d,p) basis set.[12−15] At the B3LYP/6-311++G(d,p) geometries, reaction energies were computed using the singles and doubles coupled-cluster method with a perturbative correction for connected triple substitutions [CCSD(T)] in conjunction with the Bauschlicher ANO basis set for Cr[16,17] and the cc-pVTZ set[18] for H and O. The CCSD(T) computations employed the frozen core approximation, freezing the Cr 1s2s2p3s3p and the O 1s orbitals in the correlation procedure.

A number of corrections were applied to the CCSD(T) reaction energies, including corrections for core-correlation and scalar relativistic effects as well as a basis set incompleteness correction. Coupled-cluster singles and doubles theory (CCSD), second-order Møller−Plesset perturbation theory (MP2), and Hartree−Fock (HF) theory were used for computation of these corrections as explained below.

Core-correlation effects (the effect of including the Cr 3s and 3p orbitals in the correlation procedure) were estimated using either the CCSD or the MP2 method. For H and O, the cc-pVTZ basis was employed, and for Cr, the Bauschlicher ANO basis was modified by decontracting the outermost six s, seven p, and seven d functions (producing a Cr basis with 146 basis functions). For reactions 1−3, involving the smallest species, computations were done at the CCSD level, but coupled-cluster computations were not feasible for the remaining reactions. For reactions 5 and 6, involving only closed-shell species, core-correlation effects were instead computed at the MP2 level. For these reactions, the frozen core MP2 reaction energies (computed with the basis sets employed in the CCSD(T) computations described above) lie 12.4 and 8.9 kcal mol^{-1} respectively, below their CCSD counterparts, and the MP2 level is expected to be reasonably accurate. For reaction 4, involving $Cr(OH)_5$, the MP2 method was found to be inadequate (on the basis of a very large discrepancy between the frozen core MP2 reaction energy and its CCSD counterpart when using the basis sets employed for computing CCSD(T) reaction energies) and the core-correlation correction was omitted.

Relativistic effects were estimated using the Douglas−Kroll−Hess second-order relativistic correction,[19−22] employing the relativistic cc-pVTZ_DK basis set[17,23] for H and O and the Bauschlicher ANO set with the entire s and p spaces decontracted for Cr. The MP2 level was used for reactions 5 and 6, and HF corrections were employed for the remaining reactions.

A correction for basis set incompleteness was obtained by computing reaction energies using a completely decontracted Bauschlicher ANO basis set on Cr and the aug-cc-pVQZ set[18,24] on H and O. For reactions 5 and 6, energies were computed at the MP2 level, and computations were performed at the HF level for the other reactions.

For open-shell species, unrestricted Hartree−Fock (UHF) wave functions were used throughout with the following two exceptions. First, the open-shell CCSD(T) computations were performed with the MOLPRO[25] UCCSD(T) method, which uses a high-spin restricted open-shell Hartree−Fock (ROHF) wave function reference.[26] Second, the various corrections applied to reaction 4 were computed using ROHF reference wave functions because the spin contamination in the UHF wave function for $Cr(OH)_5$ is large. For $Cr(OH)_5$, the expectation value of the S^2 operator for the UHF wave function is 1.16 (vs 0.75 for a pure doublet), whereas the spin contamination for all other species is at most 0.04. We note that the spin contamination in the open-shell B3LYP wave functions is small in all cases (0.04 or less).

Thermal corrections, $H^\circ_{298.15} - H^\circ_0$, were computed using standard formulas from statistical mechanics[27] (employing the rigid-rotor, harmonic-oscillator approximations) and using a hindered rotor treatment based on the Pitzer and Gwinn approach[28] for the vibrational modes corresponding to internal rotations of hydroxide groups.

All density functional computations and CCSD core-correlation computations, as well as MP2 calculations for the smaller chromium species, were performed with Gaussian03.[29] CCSD(T) energies were computed with MOLPRO,[25] and large MP2 computations were carried out with MPQC.[30] Relativistic computations were done using the NWChem[31] program.

3. Results and Discussion

3.1. Geometries and Frequencies. Selected B3LYP/6-311++G(d,p) optimized bond distances for the target chromium hydroxides and oxyhydroxides and the chromium-containing auxiliary species are listed in Table 3, and the optimized

TABLE 3: Selected B3LYP/6-311++G(d,p) Optimum Bond Distances for Chromium Species[a]

species	point group	r_e (Å)
CrOH (^{6}A′)	C_s	1.835
$Cr(OH)_2$ (^{5}B)	C_2	1.814
$Cr(OH)_3$ ($^4A_1$)	C_{3v}	1.785
$Cr(OH)_4$ (^{3}A″)	C_s	1.777,1.791,1.764,1.764
$Cr(OH)_5$ (^{2}A)	C_1	1.739,1.797,1.799,1.798,1.813
$Cr(OH)_6$ (^{1}A)	C_3	1.889,1.889,1.889,1.764,1.764,1.764
$CrO(OH)_4$ (^{1}A)	C_1	1.542(Cr═O),1.848,1.774,1.772,1.854
CrO_3 ($^1A_1$)	C_{3v}	1.578(Cr═O)

[a] Cr−OH distances, unless otherwise noted. For each species, the Cr−OH distances are listed as r_e(Cr−O$_n$H) in order of increasing n, where n is the number of the oxygen atoms as assigned in Figure 1.

structures are depicted in Figure 1. The complete Cartesian geometries for the investigated chromium species are available in the Supporting Information.

The CrOH and $Cr(OH)_2$ molecules have C_s and C_2 symmetry, respectively, and the symmetry of $Cr(OH)_3$, which has a nearly planar Cr−O framework, is C_{3v}. The Cr−O framework in $Cr(OH)_4$, $Cr(OH)_5$, and $Cr(OH)_6$ is nearly tetrahedral, square pyramidal and octahedral, respectively, but both bond distances and angles are distorted somewhat from these symmetries. The resulting point groups for the optimized structures are C_s, C_1, and C_3, respectively. For $CrO(OH)_4$, the located minimum has C_1 symmetry, but the Cr−O skeleton resembles a C_{4v} structure.

For the smallest hydroxides, $Cr(OH)_n$, $n = 1-3$, the Cr−O bond distance is shortened by 0.2−0.3 Å upon the addition of another hydroxide group, assuming values of 1.835, 1.814, and 1.785 Å, respectively. While the Cr−O bond distances within the molecule are the same for $Cr(OH)_2$ and $Cr(OH)_3$, the addition of further hydroxide groups causes a splitting of the Cr−O bond distances, causing both shorter and longer bond distances to appear. The Cr−O bond distances in $Cr(OH)_4$, $Cr(OH)_5$, and $Cr(OH)_6$ lie in the ranges 1.764−1.791, 1.739−1.813, and 1.764−1.889 Å, respectively. Thus, for the larger hydroxides, steric repulsion causes some Cr−O bonds to lengthen, and the addition of a hydroxide group causes the

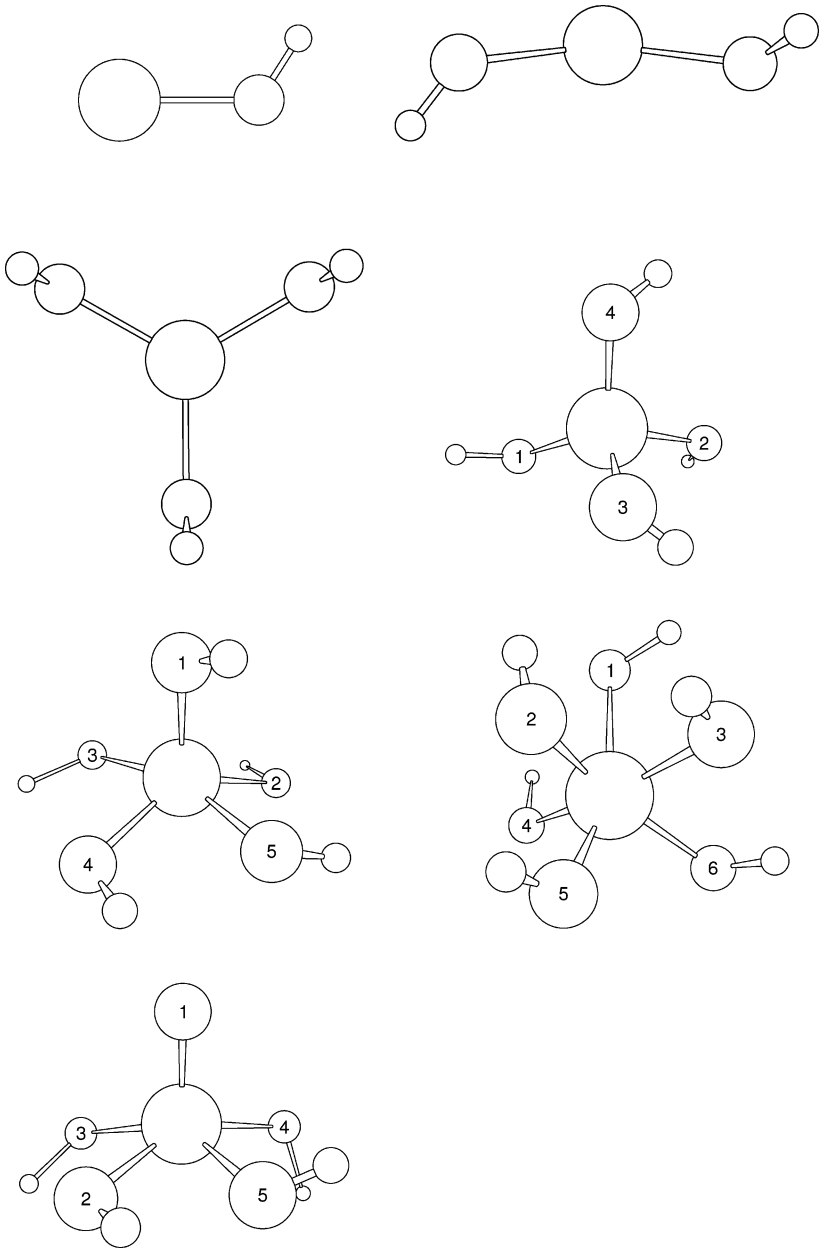

Figure 1. Computed optimum structures for chromium species $Cr(OH)_n$, $n = 1-6$, and $CrO(OH)_4$. For the larger species, for which the oxygen atoms, generally, are not symmetry-equivalent, the oxygen atoms have been numbered (cf. Table 3).

TABLE 4: Computed B3LYP/6-311++G(d,p) Harmonic Vibrational Frequencies[a]

	ω_e (cm^{-1})			
species	Cr−O framework bend/torsion	Cr−O−H bend	Cr−OH and Cr=O stretch	O−H stretch
CrOH		586	637	3858
$Cr(OH)_2$	71	453(B), 553	629, 737(B)	3892(B), 3893
$Cr(OH)_3$	164, 182(E)	606(E), 622	655, 739(E)	3856(E), 3861
$Cr(OH)_4$	131(A″), 174(A″), 175	704(A″), 730	678, 683, 738	3811, 3814,
	194, 228	747, 813	769(A″)	3824(A″), 3828
$Cr(OH)_5$	92, 223, 254, 281	787, 849, 858	568, 664, 676	3779, 3782, 3786
	311, 330, 369	928, 944	706, 745	3792, 3803
$Cr(OH)_6$	169, 173(E),277	846, 886(E)	479(E), 624	3744(E), 3749
	286(E), 386(E), 420	941(E), 1005	700, 703(E)	3748(E), 3784
$CrO(OH)_4$	81, 137, 277	771, 839, 930	527, 648, 700	3776, 3780
	310, 325, 341	1027	712, 1122	3786, 3790
	447			
CrO_3	208,376(E)		1003, 1075(E)	

[a] The symmetry (for nontotally symmetric vibrations) is given in parentheses after the frequency. [b] Modes assigned as internal rotations: $Cr(OH)_2$: 290(B), 384; $Cr(OH)_3$: 260, 379(E); $Cr(OH)_4$: 193(A″), 305(A″), 315(A″), 344; $Cr(OH)_5$: 249, 472, 548, 557, 573; $Cr(OH)_6$: 530(E), 577(E), 579, 689; $CrO(OH)_4$: 372, 416, 535, 553.

longest Cr−O bonds to be elongated further. The crowding of the oxygen atoms around the chromium atom in the larger hydroxides may be illustrated by the minimum O−O distances, which assume values of 3.1, 2.7, 2.4, and 2.3 Å in $Cr(OH)_3$, $Cr(OH)_4$, $Cr(OH)_5$, and $Cr(OH)_6$, respectively, and 2.3 Å in $CrO(OH)_4$.

For the larger chromium hydroxides, the computed structures suggest that intramolecular hydrogen bonding may be present and that the molecules adopt a configuration that maximizes the number of potential hydrogen bonds, even though the hydrogen bonds are relatively long with unfavorable bond angles of about 90−100°. Thus, in $Cr(OH)_5$, there appears to be four hydrogen bonds in the nearly planar base of the square pyramid, namely, $O_2-H\cdots O_3$, $O_3-H\cdots O_4$, $O_4-H\cdots O_5$, and $O_5-H\cdots O_2$ with hydrogen bond distances of 2.18, 2.21, 2.17, and 2.20 Å, respectively. In $Cr(OH)_6$, there are six possible hydrogen bonds, namely, three connecting the upper three symmetry-equivalent oxygen atoms (cf. Figure 1), that is, $O_1-H\cdots O_3$, $O_3-H\cdots O_2$, and $O_2-H\cdots O_1$, and three connecting the three lower oxygen atoms with the upper oxygen atoms, namely, $O_4-H\cdots O_1$, $O_5-H\cdots O_2$, and $O_6-H\cdots O_3$. The bond distances for these hydrogen bonds are 2.15 Å for the first set and 2.05 Å for the second set. In $CrO(OH)_4$, there are two relatively short O···H distances, namely, $O_2-H\cdots O_5$ (1.97 Å) and $O_3-H\cdots O_2$ (2.09 Å), and the optimum structure does not appear to maximize the number of hydrogen bonds.

For all of the investigated chromium species, extensive searches were carried out to ascertain that the optimized structures presented herein are the global minima on the respective potential energy surfaces. For several species, local minima were found, which are energetically close to the global minimum. Thus, for the smaller hydroxides, local minima were located representing a $Cr(OH)_2$ structure with the two O−H bonds pointing in the same direction and a $Cr(OH)_3$ structure with two O−H bonds above and one below the Cr−O framework. For the larger hydroxides, $Cr(OH)_5$ and $Cr(OH)_6$, numerous local minima, each with fewer hydrogen bonds than the global minimum, were located. We note that, for $CrO(OH)_4$, we were not able to locate lower-lying structures with more hydrogen bonds.

To gauge the performance of the employed computational method for obtaining structures and vibrational frequencies, a comparison may be made with available experimental data for the chromium oxides CrO, CrO_2, and CrO_3. We are not aware of any published experimental data for structures or frequencies for the chromium hydroxides or the oxyhydroxide. Structural information is available for CrO, for which the experimentally determined[32] r_e(Cr−O) value of 1.615 Å is in very good agreement with our computed value of 1.616 Å. Experimentally determined harmonic vibrational frequencies are available for CrO, CrO_2, and CrO_3. For CrO, the experimental value[33] of 846.3 cm^{-1} (Ar matrix) is in good agreement with our computed value of 867 cm^{-1}. For CrO_2, the experimental frequencies[34,35] 220 ± 20 (gas-phase), 921, and 975 (Ne matrix) cm^{-1} also agree well with our values of 225, 989, and 1032 cm^{-1}. Finally, for CrO_3, the experimentally determined value[33] of 968.4 cm^{-1} (Ar matrix) for the doubly degenerate Cr−O stretching mode is in fair agreement with our computed frequency of 1075 cm^{-1}.

The frequencies for the located optimum structures for the chromium hydroxides and the oxyhydroxide are listed in Table 4. For CrOH and $Cr(OH)_2$, our frequencies are in reasonably good agreement with frequencies computed previously[9] using gradient-corrected density functional theory and a triple-ζ basis set with diffuse functions and a single set of polarization functions on hydrogen and oxygen. For $Cr(OH)_6$ and $CrO(OH)_4$, B3LYP frequencies have previously been computed[36] using smaller basis sets than those used in the present study, and these frequencies differ significantly from our values. For the remaining higher hydroxides, we are not aware of previously determined frequencies. In the computation of thermodynamic functions for chromium species, Ebbinghaus[7] employed frequencies estimated from spectroscopic data for related vibrational modes in gaseous chromium oxides and oxyhalides as well as solid oxyhydroxides. Some of these estimated frequencies, however, deviate significantly from our computed values. In particular, Ebbinghaus used frequencies in the 410−441 cm^{-1} range for the Cr−O−H bending motions and a value of 3000 cm^{-1} for all O−H stretches. The estimated Cr−O−H bending frequencies are substantially below our computed values, especially for the larger species for which the computed frequencies lie in the 700−1000 cm^{-1} range. Additionally, the estimated frequency for the O−H stretches is considerably below our values, which all lie in the 3700−3900 cm^{-1} interval. The use of highly inaccurate frequencies may cause a large error in the zero-point vibrational energy and in the computed thermodynamic functions, especially at high temperatures.

3.2. Thermochemical Data. The computation of the heats of formation for $Cr(OH)_n$, $n = 2-6$, and $CrO(OH)_4$ is detailed in Table 5. The table lists the computed reaction energies for reactions 1−6, including the corrections for basis set incom-

TABLE 5: Evaluation of $\Delta H^\circ_{f,0}$ and $\Delta H^\circ_{f,298.15}$ for $Cr(OH)_n$, $n = 2-6$, and $CrO(OH)_4$[a]

	$Cr(OH)_2$ rxn 1	$Cr(OH)_3$ rxn 2	$Cr(OH)_4$ rxn 3	$Cr(OH)_5$ rxn 4	$Cr(OH)_6$ rxn 5	$CrO(OH)_4$ rxn 6
ΔE_{rxn}[HF]	7.71	−4.60	−50.63	132.49	−29.21	24.02
δ[CCSD]	+7.17	+18.22	+40.47	−44.51	+15.57	+1.45
δ[CCSD(T)]	+0.36	+4.62	+13.06	−11.03	+9.62	+0.78
δ[basis]	−0.30	−1.15	−2.11	−3.49	−3.91	−2.63
δ[core]	−0.37	+0.76	+1.82	[b]	+2.08	+0.90
δ[rel]	−2.53	−2.87	−3.19	+3.89	+2.06	+3.42
δ[ZPVE]	−1.06	−2.64	−4.12	−5.53	−8.07	−4.99
$\Delta H^\circ_{rxn,0}$	10.98	12.34	−4.70	71.82	−11.86	22.95
$\Delta H^\circ_{f,0}$	−72.08	−151.21	−211.97	−241.74	−235.85	−213.55
$\Delta H^\circ_{f,298.15}$	−73.19	−153.36	−214.94	−247.07	−242.64	−218.09

[a] All entries in kcal mol^{-1}. ΔE_{rxn}[HF] is the computed reaction energy at the Hartree−Fock level using the Bauschlicher ANO set for Cr and the cc-pVTZ set for O and H, and δ[CCSD] and δ[CCSD(T)] represent the increment in the reaction energy relative to the preceding level of theory. δ[basis], δ[core], δ[rel], and δ[ZPVE] denote the contributions to the reaction energy from basis set improvement, core-valence correlation, scalar relativistic effects, and zero-point vibrational energy (see text for details). $\Delta H^\circ_{f,0}$ and $\Delta H^\circ_{f,298.15}$ are computed from $\Delta H^\circ_{rxn,0}$ as described in the text. [b] No core-valence correlation correction included (see text).

pleteness, core-correlation and scalar relativistic effects, as well as the heats of formation at 0 and 298.15 K obtained using the computed reaction energies and temperature corrections as explained in section 2. Reaction energies computed at the HF level and the correlation increments at the CCSD and CCSD(T) levels are listed to illustrate the size of the correlation contributions. A large HF → CCSD or CCSD → CCSD(T) increment in the reaction energy may be indicative of large dynamic correlation effects or possible inadequacies in the single reference approach. Considering the shift in the reaction energies with improvement of the correlation method (HF → CCSD → CCSD(T)), reactions 1 and 6 display the most rapid convergence and the small correlation increments lend confidence to the accuracy of the CCSD(T) approach. The correlation shifts exhibited by reactions 2 and 5 are somewhat larger, although the observed HF → CCSD shifts of 18.2 and 15.6 kcal mol^{-1}, respectively, and CCSD → CCSD(T) increments of 4.6 and 9.2 kcal mol^{-1} are sufficiently small that the CCSD(T) method can probably be expected to provide an adequate correlation treatment. For reactions 3 and 4, the correlation contributions at the CCSD level (40.5 and −44.5 kcal mol^{-1}, respectively) are considerable, and the size of the (T) contributions (13.1 and −11.3 kcal mol^{-1}) suggests that higher-order correlation effects may not be negligible. The corrections for basis set incompleteness, core-correlation, and scalar relativistic effects are generally fairly small for all reactions, with a magnitude of 3.9 kcal mol^{-1} or less, and the size of the corrections tends to increase with the number of hydroxide groups in the target chromium species.

We note that a previous theoretical study[36] computed B3LYP structures of $Cr(OH)_6$ and $CrO(OH)_4$ and reaction energies for reactions involving these species using a 6-311G(d) basis set on Cr and a 6-311G basis on other atoms. The optimized structures resemble those computed in the present work, although both were reported to have C_1 symmetry. From the reported B3LYP reaction energies, the reaction energies for our reactions 5 and 6 can be derived and are found to be 31.3 and 50.0 kcal mol^{-1}, respectively. When computing these B3LYP reaction energies using the same basis sets (6-311G(d), 6-311G) but the geometries optimized in the present work, we obtain reaction energies of 41.2 and 55.2 kcal mol^{-1}, respectively. This difference suggests that the minima located in the present study for $Cr(OH)_6$ and $CrO(OH)_4$ correspond to lower-lying structures than those reported in ref 36. Additionally, the basis sets employed in ref 36 appear to be inadequate because they produce reaction energies that are 44 and 12 kcal mol^{-1}, respectively, above those computed with larger basis sets for reactions 5 and 6 (vide infra).

To compare energetics obtained with the B3LYP and CCSD(T) methods, we computed B3LYP reaction energies using the same basis sets as those employed for the reported coupled-cluster energies in Table 5. The computed B3LYP reaction energies are 12.0, 16.5, 2.4, 97.1, 12.2, and 37.7 kcal mol^{-1} for reactions 1−6, respectively, and the corresponding (uncorrected) CCSD(T) energies are 15.2, 18.2, 2.9, 77.0, −4.0, and 26.3 kcal mol^{-1}. Although the B3LYP reaction energies for the first three of these reactions are in good agreement with their CCSD(T) counterparts, the B3LYP values lie 11−20 kcal mol^{-1} above the CCSD(T) values for the last three reactions and the B3LYP method does not appear to be appropriate for accurate computation of reaction energies for these systems in general.

On the basis of the expected accuracy of the theoretical approach and the uncertainty in the employed experimental data, we have assigned uncertainties to our computed heats of formation. The uncertainties have been estimated as the sum of a theoretical and an experimental contribution. The theoretical contribution to the uncertainty is computed as one-half times the sum of the CCSD → CCSD(T) shift and the basis set correction (cf. Table 5) for each reaction. The experimental part of the uncertainty is computed for each reaction by adding the uncertainties in the employed heats of formation (cf. Table 2) for all species participating in the reaction. For $Cr(OH)_5$, we have added an additional contribution of 2 kcal mol^{-1} to the uncertainty because the core-correlation correction was omitted. We note that the experimental contribution to the uncertainty is considerable for some of these reactions (about 6 and 9 kcal mol^{-1} for reactions 2 and 3, respectively). However, if more accurate reference data become available, these new values can easily be employed in the computations detailed in Table 5 to yield improved heats of formation with smaller uncertainties. Our computed $\Delta H^\circ_{f,298.15}$ values for $Cr(OH)_2$, $Cr(OH)_3$, $Cr(OH)_4$, $Cr(OH)_5$, $Cr(OH)_6$, and $CrO(OH)_4$ are, in order, -73 ± 4, -153 ± 9, -215 ± 16, -247 ± 13, -243 ± 8, and -218 ± 3 kcal mol^{-1}. These values may be compared with previously obtained experimental values and a single value obtained by theory (cf. Table 1). For $Cr(OH)_2$, our value is in excellent agreement with the previously computed[9] $\Delta H^\circ_{f,298.15}$ value of -73.9 ± 2.9 kcal mol^{-1} obtained from bond dissociation energies computed using the CCSD(T) method in conjunction with the G2 and PCI-X extrapolation schemes, and our value also agrees reasonably well with the experimental value of -78.1 ± 2.6 kcal mol^{-1}. For $Cr(OH)_3$, the experimental $\Delta H^\circ_{f,298.15}$ value of -145.7 ± 3.1 is in fair agreement with the computed value, and for $CrO(OH)_4$, there is good agreement between theory and the reported experimental value of −220

kcal mol^{-1}. The largest discrepancies between theory and experiment are found for the larger hydroxides, $Cr(OH)_4$, $Cr(OH)_5$, and $Cr(OH)_6$, for which the reported experimental values of -202.9 ± 3.5, -218, and -229 kcal mol^{-1} (the latter two of which were reported to be lower limits) lie above the computed values by 12, 29, and 14 kcal mol^{-1}, respectively.

Considering that all of the previously reported experimentally derived thermochemical data for the chromium species of interest in this work (cf. Table 1) are estimated values obtained from heats of formation for chromium halides and oxyhalides by using assumptions of linear relationships between bond strengths for different ligands,[7,8] we believe our computed values for $Cr(OH)_5$ and $Cr(OH)_6$ to be the best values currently available and a resolution of the discrepancies between experiment and theory for the larger hydroxides would probably require determination of more accurate experimental heats of formation for $Cr(OH)_4-Cr(OH)_6$.

For the investigated chromium species, polynomial fits were made for the heat capacity (C_p), enthalpy ($H°$), and entropy ($S°$) as a function of temperature. Fits were performed over the 100−1000 and 1000−3000 K temperature ranges, using C_p, $H°$, and $S°$ values computed at 100° intervals. These fits, which can be used with the CHEMKIN software package,[11] are defined by

$$\frac{C_p}{R} = a_1 + a_2T + a_3T^2 + a_4T^3 + a_5T^4 \qquad (7)$$

$$\frac{H°}{RT} = a_1 + \frac{a_2}{2}T + \frac{a_3}{3}T^2 + \frac{a_4}{4}T^3 + \frac{a_5}{5}T^4 + \frac{a_6}{T} \qquad (8)$$

$$\frac{S°}{R} = a_1 \ln T + a_2T + \frac{a_3}{2}T^2 + \frac{a_4}{3}T^3 + \frac{a_5}{4}T^4 + a_7 \qquad (9)$$

where $H° = H°(T) - H°(298) + \Delta H_f°(298)$. $\Delta H_f°(298)$ designates the species heat of formation at 298 K and $H°(T)$ and $H°(298)$ represent the standard enthalpy at temperature T and at 298 K, respectively. The fitted coefficients are available in the Supporting Information and also on the World Wide Web.[37]

4. Concluding Remarks

We have computed the thermochemistry of the chromium hydroxides $Cr(OH)_n$, $n = 2-6$, and the oxyhydroxide $CrO(OH)_4$ using high-level ab initio methods. Heats of formation were obtained from isogyric reaction energies computed at the CCSD(T) level of theory using large basis sets and including corrections for core-valence correlation, scalar relativistic effects, and basis set incompleteness. Optimum geometries and harmonic vibrational frequencies were determined with the B3LYP method using basis sets of triple-ζ quality including polarization and diffuse functions. Heats of formation were obtained at both 0 and 298.15 K using temperature corrections computed from thermodynamic functions determined using the B3LYP geometries and frequencies. Polynomial fits were performed for the heat capacity and the standard enthalpy and entropy over the 100−3000 K temperature range. Our computed $\Delta H°_{f,298.15}$ values for the hydroxides $Cr(OH)_n$, $n = 2-6$, are, in order of increasing n, -73 ± 4, -153 ± 9, -215 ± 16, -247 ± 13, and -243 ± 8 kcal mol^{-1}, and the value obtained for $CrO(OH)_4$ is -218 ± 3 kcal mol^{-1}. While there is reasonable agreement between previously determined experimental values and our computed values for the smaller hydroxides $Cr(OH)_2$ and $Cr(OH)_3$ and good agreement for $CrO(OH)_4$, discrepancies in the range of 12−29 kcal mol^{-1} are found between theory and experiment for the larger hydroxides $Cr(OH)_4-Cr(OH)_6$. For the larger hydroxides, we suggest that a revision of the experimental values may be appropriate.

Acknowledgment. Funding for this work was provided by the U.S. Department of Energy Industrial Technologies Program and Industrial Materials for the Future Program.

Supporting Information Available: Cartesian coordinates for the B3LYP/6-311++G(d,p) optimum structures, energies computed at the HF, CCSD, and CCSD(T) levels, and fitted coefficients for polynomial fits for the heat capacity, enthalpy, and entropy for $Cr(OH)_n$, $n = 2-6$, and $CrO(OH)_4$. This material is available free of charge via the Internet at http://pubs.acs.org.

References and Notes

(1) Hilpert, K.; Das, D.; Miller, M.; Peck, D. H.; Weiss, R. *J. Electrochem. Soc.* **1996**, *143*, 3642.
(2) Fergus, J. W. *Mater. Sci. Eng., A* **2005**, *397*, 271.
(3) O'Leary, J. R.; Kunz, R. G.; von Alten, T. R. *Environ. Prog.* **2004**, *23*, 194.
(4) Bailey, J. *J. Electrochem. Soc.* **1997**, *144*, 3568.
(5) Nielsen, I. M. B.; Allendorf, M. D. *J. Phys. Chem. A* **2005**, *109*, 928.
(6) Opila, E. J.; Myers, D. L.; Jacobson, N. S.; Nielsen, I. M. B.; Johnson, D. F.; Olminsky, J. K.; Allendorf, M. D. *J. Phys. Chem. A*, to be submitted for publication.
(7) Ebbinghaus, B. B. *Combust. Flame* **1993**, *93*, 119.
(8) Ebbinghaus, B. B. *Combust. Flame* **1995**, *101*, 311.
(9) Espelid, Ø.; Børve, K. J.; Jensen, V. R. *J. Phys. Chem. A* **1998**, *102*, 10414.
(10) See ref 9 and references therein.
(11) Kee, R. J.; Rupley, F. M.; Miller, J. A.; Coltrin, M. E.; Grcar, J. F.; Meeks, E.; Moffat, H. K.; Lutz, A. E.; Dixon-Lewis, G.; Smooke, M. D.; Warnatz, J.; Evans, G. H.; Larson, R. S.; Mitchell, R. E.; Petzold, L. R.; Reynolds, W. C.; Caracotsios, M.; Stewart, W. E.; Glarborg, P.; Wang, C.; Adignun, O. *Chemkin Collection*, release 3.6 ed.; Reaction Design, Inc.: San Diego, CA, 2000.
(12) Frisch, M. J.; Pople, J. A.; Binkley, J. S. *J. Chem. Phys.* **1984**, *80*, 3265.
(13) Hay, P. J. *J. Chem. Phys.* **1977**, *66*, 4377.
(14) Wachters, A. J. H. *J. Chem. Phys.* **1970**, *52*, 1033.
(15) For Cr, the 6-311++G(d,p) set is the Wachters−Hay all-electron basis using the scaling factors of Raghavachari and Trucks.
(16) Bauschlicher, C. W. *Theor. Chim. Acta* **1995**, *92*, 183.
(17) Obtained from the Extensible Computational Chemistry Environment Basis Set Database, version 1/02/02, as developed and distributed by the Molecular Science Computing Facility, Environmental and Molecular Sciences Laboratory which is part of the Pacific Northwest Laboratory, P.O. Box 999, Richland, WA 99352, and funded by the U.S. Department of Energy. The Pacific Northwest Laboratory is a multiprogram laboratory operated by the Battelle Memorial Institue for the U.S. Department of Energy under Contract DE-AC06-76RLO 1830. Contact David Feller or Karen Schuchardt for further information.
(18) Dunning, T. H., Jr. *J. Chem. Phys.* **1989**, *90*, 1007.
(19) Douglas, M.; Kroll, N. M. *Ann. Phys.* **1974**, *82*, 89.
(20) Hess, B. A. *Phys. Rev. A* **1985**, *32*, 756.
(21) Hess, B. A. *Phys. Rev. A* **1986**, *33*, 3742.
(22) Jansen, G.; Hess, B. A. *Phys. Rev. A* **1989**, *39*, 6016.
(23) de Jong, W. A.; Harrison, R. J.; Dixon, D. A. *J. Chem. Phys.* **2001**, *114*, 48.
(24) Kendall, R. A.; Dunning, T. H., Jr.; Harrison, R. J. *J. Chem. Phys.* **1992**, *96*, 6796.
(25) MOLPRO, a package of ab initio programs designed by Werner, H.-J. and Knowles, P. J., version 2002.3, Amos, R. D.; Bernhardsson, A.; Berning, A.; Celani, P.; Cooper, D. L.; Deegan, M. J. O.; Dobbyn, A. J.; Eckert, F.; Hampel, C.; Hetzer, G.; Knowles, P. J.; Korona, T.; Lindh, R.; Lloyd, A. W.; McNicholas, S. J.; Manby, F. R.; Meyer, W.; Mura, M. E.; Nicklass, A.; Palmieri, P.; Pitzer, R.; Rauhut, G.; Schütz, M.; Schumann, U.; Stoll, H.; Stone, A. J.; Tarroni, R.; Thorsteinsson, T.; Werner, H.-J.
(26) Knowles, P. J.; Hampel, C.; Werner, H.-J. *J. Chem. Phys.* **1993**, *99*, 5219.
(27) McQuarrie, D. A. *Statistical Mechanics*; Harper & Row: New York, 1976.
(28) Pitzer, K. S.; Gwinn, W. D. *J. Chem. Phys.* **1942**, *10*, 428.
(29) Frisch, M. J.; Trucks, G. W.; Schlegel, H. B.; Scuseria, G. E.; Robb, M. A.; Cheeseman, J. R.; Montgomery, J. A., Jr.; Vreven, T.; Kudin, K. N.; Burant, J. C.; Millam, J. M.; Iyengar, S. S.; Tomasi, J.; Barone, V.; Mennucci, B.; Cossi, M.; Scalmani, G.; Rega, N.; Petersson, G. A.; Nakatsuji, H.; Hada, M.; Ehara, M.; Toyota, K.; Fukuda, R.; Hasegawa, J.;

Ishida, M.; Nakajima, T.; Honda, Y.; Kitao, O.; Nakai, H.; Klene, M.; Li, X.; Knox, J. E.; Hratchian, H. P.; Cross, J. B.; Bakken, V.; Adamo, C.; Jaramillo, J.; Gomperts, R.; Stratmann, R. E.; Yazyev, O.; Austin, A. J.; Cammi, R.; Pomelli, C.; Ochterski, J. W.; Ayala, P. Y.; Morokuma, K.; Voth, G. A.; Salvador, P.; Dannenberg, J. J.; Zakrzewski, V. G.; Dapprich, S.; Daniels, A. D.; Strain, M. C.; Farkas, O.; Malick, D. K.; Rabuck, A. D.; Raghavachari, K.; Foresman, J. B.; Ortiz, J. V.; Cui, Q.; Baboul, A. G.; Clifford, S.; Cioslowski, J.; Stefanov, B. B.; Liu, G.; Liashenko, A.; Piskorz, P.; Komaromi, I.; Martin, R. L.; Fox, D. J.; Keith, T.; Al-Laham, M. A.; Peng, C. Y.; Nanayakkara, A.; Challacombe, M.; Gill, P. M. W.; Johnson, B.; Chen, W.; Wong, M. W.; Gonzalez, C.; Pople, J. A. *Gaussian 03*, revision C.02; Gaussian, Inc.: Wallingford, CT, 2004.

(30) Janssen, C. L.; Nielsen, I. B.; Leininger, M. L.; Valeev, E. F.; Seidl, E. T. *The Massively Parallel Quantum Chemistry Program (MPQC)*, version 2.3.0-alpha; Sandia National Laboratories: Livermore, CA, 2005 (http://www.mpqc.org).

(31) Straatsma, T. P.; Aprà, E.; Windus, T. L.; Bylaska, E. J.; de Jong, W.; Hirata, S.; Valiev, M.; Hackler, M.; Pollack, L.; Harrison, R.; Dupuis, M.; Smith, D. M. A.; Nieplocha, J.; Tipparaju V.; Krishnan, M.; Auer, A. A.; Brown, E.; Cisneros, G.; Fann, G.; Früchtl, H.; Garza, J.; Hirao, K.; Kendall, R.; Nichols, J.; Tsemekhman, K.; Wolinski, K.; Anchell, J.; Bernholdt, D.; Borowski, P.; Clark, T.; Clerc, D.; Dachsel, H.; Deegan, M.; Dyall, K.; Elwood, D.; Glendening, E.; Gutowski, M.; Hess, A.; Jaffe, J.; Johnson, B.; Ju, J.; Kobayashi, R.; Kutteh, R.; Lin, Z.; Littlefield, R.; Long, X.; Meng, B.; Nakajima, T.; Niu, S.; Rosing, M.; Sandrone, G.; Stave, M.; Taylor, H.; Thomas, G.; van Lenthe, J.; Wong, A.; Zhang, Z. *NWChem, A Computational Chemistry Package for Parallel Computers*, version 4.6; Pacific Northwest National Laboratory: Richland, WA, 2004. Kendall, R. A.; Aprà, E.; Bernholdt, D. E.; Bylaska, E. J.; Dupuis, M.; Fann, G. I.; Harrison, R. J.; Ju, J.; Nichols, J. A.; Nieplocha, J.; Straatsma, T. P.; Windus, T. L.; Wong, A. T. High Performance Computational Chemistry: an Overview of NWChem a Distributed Parallel Application. *Comput. Phys. Commun.* **2000**, *128*, 260−283.

(32) Huber, K. P.; Herzberg, G. (data prepared by Gallagher, J. W.; Johnson, R. D., III). Constants of Diatomic Molecules. In *NIST Chemistry WebBook*; NIST Standard Reference Database Number 69; Mallard, W. G., Linstrom, P. J., Eds.; National Institute of Standards and Technology: Gaithersburg MD, February 2000 (http://webbook.nist.gov).

(33) Chertihin, G. V.; Bare, W. D.; Andrews, L. *J. Chem. Phys.* **1997**, *107*, 2798.

(34) Wenthold, P. G.; Jonas, K.-L.; Lineberger, W. C. *J. Chem. Phys.* **1997**, *106*, 9961.

(35) Zhou, M.; Andrews, L. *J. Chem. Phys.* **1999**, *111*, 4230.

(36) Johnson, J. R. T.; Panas, I. *Inorg. Chem.* **2000**, *39*, 3181.

(37) http://www.ca.sandia.gov/HiTempThermo/.

(38) *JANAF Thermochemical Tables*, 3rd ed.; *J. Phys. Chem. Ref. Data* 1985; Vol. 14, Supplement No. 1.